Assessment of Conventional Density Functional Schemes for Computing the Polarizabilities and hyperpolarizabilities of Conjugated Oligomers: An Ab Initio Investigation of Polyacetylene Chains

Champagne, B.; Perpète, E.A.; van Gisbergen, S.J.A.; Baerends, E.J.; Snijders, J.G.; Soubra-Ghaoui, C.; Robins, K.A.; Kirtman, B.

published in
Journal of Chemical Physics
1998

DOI (link to publisher)
10.1063/1.477731

document version
Publisher's PDF, also known as Version of record

Vibrational second hyperpolarizability of $CH_{4-n}F_n$ molecules with $n=0-4$

Olivier Quinet and Benoît Champagne
Laboratoire de Chimie Théorique Appliquée, Facultés Universitaires Notre-Dame de la Paix, rue de Bruxelles, 61, B-5000 Namur, Belgium

(Received 3 June 1998; accepted 11 September 1998)

The frequency-dependent vibrational second hyperpolarizability of $CH_{4-n}F_n$ molecules with $n=0-4$ has been computed for the most common nonlinear optical (NLO) processes by adopting the perturbation approach due to Bishop and Kirtman [J. Chem. Phys. **95**, 2646 (1991)]. These calculations have been performed by using the Sadlej atomic basis set with the Hartree-Fock technique as well as with the Møller-Plesset second order perturbation theory (MP2) procedure. The inclusion of electron correlation and of the first-order mechanical and electrical anharmonicities turn out to be of quantitative importance for most quantities. In particular, it permits us to improve the agreement with the experimental data for the difference between the anisotropic dc-Kerr and mean electric-field-induced second harmonic generation (ESHG) vibrational second hyperpolarizability of CF_4. With the exception of the small ESHG vibrational second hyperpolarizability the infinite optical frequency method turns out to be a satisfactory approximation for evaluating the vibrational NLO responses. © *1998 American Institute of Physics.* [S0021-9606(98)30347-5]

I. INTRODUCTION

In 1984 Elliott and Ward[1] have compared the second hyperpolarizabilities, γ, of methane and fluorinated methanes derived from third-harmonic generation (THG),[2] electric-field-induced second harmonic generation (ESHG),[3,4] and dc-Kerr[5,6] measurements. After removing the frequency-dispersion of the electronic contribution, γ^e, they ascribed the significant differences between the third-order nonlinear responses to vibrational contributions, γ^v. They showed for CH_4 and CF_4 that spectroscopic ''semiempirical'' evaluations of γ^v at the double harmonic oscillator level of approximation were consistent with the differences obtained from the nonlinear optical (NLO) measurements. Here, we evaluate γ^v of methane and the fluorinated methanes by using the perturbative approach originally proposed by Bishop and Kirtman.[7] We also explore the replacement of the optical frequency (ω) by $\omega\rightarrow\infty$, i.e., within the so-called enhanced[1] or infinite optical frequency[8] approximation. These theoretical calculations are carried out at the Hartree-Fock (HF) level of approximation as well as within the Møller-Plesset perturbation theory limited to second order (MP2). Our values are compared with recent experimental[9–12] and theoretical[13–19] values.

When static and dynamic external electric fields are applied to a molecule, the electrons and nuclei rearrange in order to minimize the field-dependent energy. The fields induce modifications of the dipole moment of which the linear and nonlinear dependencies as a function of the field amplitude are described by the linear polarizability (α), first (β) and second (γ) hyperpolarizabilities. Several phenomena given in increasing order of response time occur: (i) the electronic distribution is modified, (ii) the equilibrium geometry of the ground state is perturbed and the molecule possibly adopts a new configuration, and (iii) the molecule rotates in order to align its dipole moment—or induced dipole moment—parallel to the external field. In condensed media, phase transitions and temperature effects also occur if the field is applied for a sufficiently long time. In material science, the rotational and temperature effects are mainly seen as side-effects to the NLO responses because they are too slow to be of practical interest. On the other hand, the electronic and vibrational effects can be maximized to optimize the NLO response. It is reasonable to consider that the external electric fields act sequentially upon the electronic and nuclear motions and therefore to adopt the so-called clamped-nucleus (CN) approximation.[20] Within this picture, the electric fields modify the electronic distribution with which is associated the electronic contribution to the (hyper)polarizabilities, (P^e, with $P=\alpha$, β, or γ). Then, the nuclei move on the field-perturbed potential energy surface to reach their field-dependent equilibrium geometry. The variation of the dipole moment upon the field-induced nuclear relaxation is associated with the nuclear relaxation contribution (P^{nr}) whereas the curvature term (P^{curv}) originates from the field-dependence of the zero-point vibrational energy.

It has been shown for diatomic[21] and polyatomic molecules[22] that the curvature term contains the zero-point vibrational averaging (ZPVA) correction to the properties, $\Delta P^e(\mathrm{ZPVA})$. In the time-dependent perturbative approach due to Bishop and Kirtman[7,22] the P^e and $\Delta P^e(\mathrm{ZPVA})$ contributions are treated together whereas the remaining terms form the pure vibrational contribution denoted P^v. Such separation into electronic and vibrational contributions is appealing when analyzing their frequency dispersion. On the one hand, the dispersion of the $P^e+\Delta P^e(\mathrm{ZPVA})$ contribution follows a power series expansion in the square of the optical frequencies. These optical effects have been investigated almost exclusively for the P^e contribution alone,[23–25] but are equally appropriate for $\Delta P^e(\mathrm{ZPVA})$ (Ref. 16) as can be seen from the analytic expressions of the latter. On the other hand, since their poles are linear combinations of harmonic normal mode vibrational frequencies, the vibrational

contribution presents large variations in the infrared region. As a result, it becomes less and less frequency-dependent as the frequency increases. This fact justifies the interest for the simple infinite optical frequency method.[8,15]

Since the work of Elliott and Ward,[1] the importance of γ^v in small molecules has been tackled extensively by both the experimentalits and theoreticians. γ^v has a typical frequency-dispersion and can be distinguished from its electronic counterpart. γ^v can also be related to spectroscopic measurements. By taking advantage of both the experimental and theoretical developments for determining very accurate γ values, many authors have compared electronic to vibrational second hyperpolarizabilities for several dozens of small molecules as a function of the NLO process and the optical frequencies. The most recent review due to Bishop[26] focuses upon these aspects but also points out the role of the vibrational hyperpolarizability contributions in NLO materials. This later aspect has been considered in details in another review paper by Kirtman and Champagne[27] who have highlighted for organic conjugated compounds the interplay between the electronic and nuclear nonlinear responses as a function of the chemical nature of the chromophore, its size, its charge state, as well as of the surrounding medium.

The present work addresses the importance of the vibrational contribution to the third-order NLO responses of five molecules. Its purpose is to compare the computed γ^v values, including or not the effects of electron correlation to the available experimental data. Where no experimental values are available, our purpose is to provide information which, from the dispersion curve of a given NLO process, will help in estimating the dispersion curve for other processes. A secondary purpose is the demonstration that for small polyatomic molecules one can perform calculations of γ^v by including electron correlation corrections, that the approximation of the infinite optical frequency is satisfactory, and that these electron correlation effects are important in several instances.

II. METHOD

The field-dependence of the dipole moment due to external static and/or dynamic (of frequency ω_i) electric fields (E) is described by a Taylor series expansion where the $K^{(n)}$ factors are such that the nonlinear responses converge towards the same static limit,

$$\mu_\zeta(\omega_\sigma)=\mu_\zeta^0+\sum_\eta \alpha_{\zeta\eta}(-\omega_\sigma;\omega_1)E_\eta(\omega_1)+\frac{1}{2!}K^{(2)}\sum_{\eta\xi}\beta_{\zeta\eta\xi}(-\omega_\sigma;\omega_1,\omega_2)E_\eta(\omega_1)E_\xi(\omega_2)+\frac{1}{3!}K^{(3)}\sum_{\eta\xi\chi}\gamma_{\zeta\eta\xi\chi}(-\omega_\sigma;\omega_1,\omega_2,\omega_3)\times E_\eta(\omega_1)E_\xi(\omega_2)E_\chi(\omega_3)+\cdots, \quad (1)$$

where $\omega_\sigma=\Sigma_i\omega_i$ and the summations over the field indices η, ξ and χ, associated with the Cartesian coordinates. μ_ζ^0 is one component of the permanent dipole moment. The static, dc-Kerr, ESHG, THG, and DFWM responses are therefore given by $\gamma(0;0,0,0)$, $\gamma(-\omega;\omega,0,0)$, $\gamma(-2\omega;\omega,\omega,0)$, $\gamma(-3\omega;\omega,\omega,\omega)$ and $\gamma(-\omega;\omega,-\omega,\omega)$, respectively. DFWM stands for degenerate four-wave mixing.

From the exact summation-over-states (SOS) expressions, Bishop and Kirtman[7] have derived the CN vibrational hyperpolarizability expressions and have worked out compact expressions under nonresonant conditions. In their notation, the tensor components of γ^v are expressed as

$$\gamma^v_{\zeta\eta\xi\chi}(-\omega_\sigma;\omega_1,\omega_2,\omega_3)=[\alpha^2]+[\mu\beta]+[\mu^2\alpha]+[\mu^4], \quad (2)$$

where the square brackets represent summations over the vibrational excited states of quotients in which the numerator is a product of vibrational transition moments of static electronic properties (μ^e,α^e,β^e), and the denominator contains vibrational and optical frequencies. For polyatomic molecules perturbation theory has to be applied to determine the square-bracketed contributions.[7,22] The electronic properties as well as the vibrational potential (and consequently the vibrational wave functions) are expanded as Taylor series in the normal coordinates. The truncation of these expansions determines the level of electrical and mechanical anharmonicity, respectively. The interested reader is referred to Refs. 7 and 22 for details of the derivations and expressions. When including mechanical and electrical anharmonicities up to first order, the tensor components of γ^v read as

$$\gamma^v_{\zeta\eta\xi\chi}(-\omega_\sigma;\omega_1,\omega_2,\omega_3)=[\alpha^2]^{0,0}+[\mu\beta]^{0,0}+[\mu^2\alpha]^{1,0}+[\mu^2\alpha]^{0,1}, \quad (3)$$

where, e.g., in $[\mu^2\alpha]^{n,m}$, n is the order of electrical anharmonicity (the number of times a second derivative of an electronic property appears) and m is the order of mechanical anharmonicity (the number of times a cubic force constant, F_{abc}, appears). Following Ref. 7, the square brackets of Eqs. (3) are developed as summation-over-modes (SOM) expressions

$$[\alpha^2]^{0,0}=\frac{1}{8}\sum P_{-\sigma,1,2,3}\sum_a \frac{\left(\frac{\partial\alpha^e_{\zeta\eta}}{\partial Q_a}\right)_0\left(\frac{\partial\alpha^e_{\xi\chi}}{\partial Q_a}\right)_0}{\omega_a^2-(\omega_2+\omega_3)^2}, \quad (4)$$

$$[\mu\beta]^{0,0}=\frac{1}{6}\sum P_{-\sigma,1,2,3}\sum_a \frac{\left(\frac{\partial\mu^e_{\zeta}}{\partial Q_a}\right)_0\left(\frac{\partial\beta^e_{\eta\xi\chi}}{\partial Q_a}\right)_0}{(\omega_a^2-\omega_\sigma^2)}, \quad (5)$$

$$[\mu^2\alpha]^{1,0}=\frac{1}{4}\sum P_{-\sigma,1,2,3}\times\sum_a\sum_b \frac{\left(\frac{\partial\mu^e_{\zeta}}{\partial Q_a}\right)_0\left(\frac{\partial^2\alpha^e_{\eta\xi}}{\partial Q_a Q_b}\right)_0\left(\frac{\partial\mu^e_{\chi}}{\partial Q_b}\right)_0}{(\omega_a^2-\omega_\sigma^2)(\omega_b^2-\omega_3^2)}+2\frac{\left(\frac{\partial\mu^e_{\zeta}}{\partial Q_a}\right)_0\left(\frac{\partial^2\mu^e_{\eta}}{\partial Q_a Q_b}\right)_0\left(\frac{\partial\alpha^e_{\xi\chi}}{\partial Q_b}\right)_0}{(\omega_a^2-\omega_\sigma^2)(\omega_b^2-(\omega_2+\omega_3)^2)}, \quad (6)$$

$$[\mu^2\alpha]^{0,1}=-\frac{1}{4}\sum P_{-\sigma,1,2,3}\sum_a\sum_b\sum_c F_{abc}\times\frac{\left(\frac{\partial\mu^e_\zeta}{\partial Q_a}\right)_0\left(\frac{\partial\mu^e_\eta}{\partial Q_b}\right)_0\left(\frac{\partial\alpha^e_{\xi\chi}}{\partial Q_c}\right)_0}{(\omega_a^2-\omega_\sigma^2)(\omega_b^2-\omega_1^2)(\omega_c^2-(\omega_2+\omega_3)^2)}, \tag{7}$$

where the sums run over the $3N-6$ ($3N-5$ for linear molecules) normal mode coordinates, $\Sigma P_{-\sigma,1,2,3}$ is the summation over the 24 permutations of the pairs $(-\omega_\sigma,\zeta)$, (ω_1,η), (ω_2,ξ) and (ω_3,χ), and Q_a is the normal mode coordinate having the frequency $\omega_a=2\pi\nu_a$. $(\partial P^e/\partial Q_a)_0$ and $(\partial^2 P^e/\partial Q_a\partial Q_b)_0$ are partial first and second derivatives of the static electronic property $P^e[=\mu^e,\alpha^e,\beta^e]$ with respect to the normal coordinates Q_a and Q_b, evaluated at the equilibrium nuclear configuration (subscript 0). Provided the parameters have been determined, Eqs. (4)–(7) give access to γ^ν for any NLO process and set of frequencies.

Within the infinite-frequency approximation, one assumes that the vibrational frequencies are at least one order of magnitude smaller than the optical frequencies or, in other words that the dispersion of the dynamic vibrational hyperpolarizability for a given process is small in the optical wavelength domain. Within this approximation, for the diagonal components of γ as well as for the parallel or isotropically average, $\gamma_\parallel=\overline{\gamma}=[\gamma_{\xi\xi\eta\eta}+\gamma_{\xi\eta\xi\eta}+\gamma_{\xi\eta\eta\xi}]/15$, quantity, (Einstein convention) the vibrational contributions to the various third-order NLO processes are expressed as simple fractional multiples of the corresponding quantities in the static limit,

$$\text{dc-Kerr:}\quad \gamma^\nu(-\omega;\omega,0,0)_{\omega\to\infty}=\frac{1}{3}[\alpha^2]^{0,0}_{\omega=0}+\frac{1}{2}[\mu\beta]^{0,0}_{\omega=0}+\frac{1}{6}[\mu^2\alpha]^{1,0}_{\omega=0}+\frac{1}{6}[\mu^2\alpha]^{0,1}_{\omega=0}, \tag{8}$$

$$\text{ESHG:}\quad \gamma^\nu(-2\omega;\omega,\omega,0)_{\omega\to\infty}=\frac{1}{4}[\mu\beta]^{0,0}_{\omega=0}, \tag{9}$$

$$\text{DFWM:}\quad \gamma^\nu(-\omega;\omega,\omega,-\omega)_{\omega\to\infty}=\frac{2}{3}[\alpha^2]^{0,0}_{\omega=0}, \tag{10}$$

$$\text{THG:}\quad \gamma^\nu(-3\omega;\omega,\omega,\omega)_{\omega\to\infty}=0, \tag{11}$$

where, e.g., $[\alpha^2]^{0,0}_{\omega=0}$ is obtained from Eq. (4) by setting $\omega_1=\omega_2=\omega_3=\omega_\sigma=0$.

For the nondiagonal components as well as for the perpendicular quantity, $\gamma^K_\perp=[2\gamma_{\xi\xi\eta\eta}(-\omega;\omega,0,0)-\gamma_{\xi\eta\xi\eta}(-\omega;\omega,0,0)]/15$, and therefore for the anisotropic Kerr constant, $\gamma^K=3/2(\gamma^K_\parallel-\gamma^K_\perp)$, where $\gamma^K_\parallel=\gamma_\parallel(-\omega;\omega,0,0)$, such simple relations between the static and infinite frequency terms are no longer valid. Indeed, it is still possible to express the individual tensor elements of the infinite-frequency vibrational NLO responses as simple fractional multiples of the corresponding static tensor but the multiplicative factors can vary when changing or permuting the indices.

Bishop and Dalskov[15] have recently concluded that the infinite optical frequency approximation is satisfactory for the dynamic γ^ν of CH_4, NH_3, H_2O, HF, and CO_2, whereas in the static limit, higher-order terms can be substantial.[15,18] Finally, it is important to stress that Eqs. (8)–(11) are identical to those obtained for the nuclear relaxation contribution to γ from a finite-field approach.[8,18]

III. COMPUTATIONAL PROCEDURE

All the calculations have been performed by using the GAUSSIAN94 series of programs[28] and the Sadlej atomic basis set.[29] Results for CH_4 (Refs. 14 and 15) and CF_4 (Ref. 30) obtained with more extended basis sets show very little variations of γ^ν with respect to the Sadlej basis set and justify therefore our choice. At the Hartree-Fock level, GAUSSIAN94 finds, analytically by adopting coupled Hartree-Fock procedures,[31] the force constants, the vibrational frequencies and normal modes, the polarizability and first hyperpolarizability as well as the derivatives of the dipole moment and polarizability with respect to the normal coordinates. At the MP2 level, analytical procedures provide the force constants, the vibrational frequencies and normal modes, the polarizability as well as the derivatives of the dipole moment with respect to the normal coordinates. Since the various dipole and (hyper)polarizability derivatives are very sensitive to the geometry, a very tight convergence threshold was chosen for the geometry optimization: limiting the residual forces on the atoms at 1.5×10^{-6} hartree/bohr or hartree/rad. The quantities necessary to evaluate Eqs. (4)–(7) which cannot be obtained from an analytical scheme were calculated by adopting numerical finite difference methods, the accuracy of which was improved by employing the Romberg procedure.[32] This removes contaminations from higher-order terms. For instance, the $(\partial\beta^e/\partial Q)_0$ quantities were evaluated by performing β^e calculations for the different structures obtained by the addition of different fractions of the normal coordinate to the equilibrium geometry. In order to reach a sufficient accuracy (of the order of 0.1–1.0 a.u.) for $[\mu\beta]^{0,0}_{\omega=0}$ it was sufficient to use distortions such that the amplitude of the Cartesian displacements is 0.050 Å and 0.025 Å together with one Romberg iteration.[33] A similar strategy was used to evaluate the cubic force constants from the harmonic force constants of distorted structures whereas the evaluation of the double derivatives with respect to the normal coordinates level required the use of a double numerical finite distortion procedure. For computing $(\partial\beta^e/\partial Q)_0$ at the MP2 level, in addition to the finite field procedure[34] used to compute β^e from the field-dependent α^e values, a finite distortion procedure was employed to differentiate β^e with respect to the normal coordinates. The various parameters entering in these finite difference schemes (i.e., the accuracy on the density matrix, on the energy, and on their derivatives, the amplitude of the distortions and of the external electric field as well as the number of Romberg iterations) have been optimized and the corresponding values compared to available analytical results to ensure that the accuracy on the total γ^ν is better than 1.0–2.0 a.u. (Ref. 35).

In order to address the importance of the vibrational con-

TABLE I. RHF- and MP2-optimized geometrical parameters in Å (bond length) and deg (bond angle) in comparison with experiment.

	CH_4	CH_3F	CH_2F_2	CHF_3	CF_4
		RHF			
R_e(C-H)	1.0900	1.0887	1.0868	1.0839	/
R_e(C-F)	/	1.3637	1.3355	1.3133	1.2979
α(H-C-H)	109.47	109.98	112.64	/	/
α(H-C-F)	/	108.95	108.97	110.47	/
α(F-C-F)	/	/	108.23	108.46	109.47
		MP2			
R_e(C-H)	1.1005	1.1014	1.1007	1.0984	/
R_e(C-F)	/	1.3946	1.3649	1.3412	1.3254
α(H-C-H)	109.47	110.17	113.71	/	/
α(H-C-F)	/	108.77	108.71	110.60	/
α(F-C-F)	/	/	108.17	108.32	109.47
		Experiment			
R_e(C-H)	1.0858[a], 1.0870[b]	1.095[c]	1.093[d]	1.098[e]	/
R_e(C-F)	/	1.382[c]	1.357[d]	1.332[e]	1.323[f]
α(H-C-H)	109.47	110.45[c]	113.7[d]	/	/
α(H-C-F)	/	108.47[c]	108.7[d]	110.1[e]	/
α(F-C-F)	/	/	108.3[d]	108.8[e]	109.47

[a]D. L. Gray and A. G. Robiette, Mol. Phys. **37**, 1901 (1979).
[b,c,d,e,f]*Handbook of Chemistry and Physics*, 78th ed., edited by D. R. Lide (CRC Press, Boca Raton, 1997–1998), pp. 9-34, 9-35, 9-30, 9-32, and 9-17, respectively.

tribution, we have also computed its electronic counterpart in the static limit for both the Hartree-Fock and MP2 wave functions. The various γ tensor components have been calculated by employing a finite field procedure[34] where the electronic polarizability tensor of the molecular structure in its ground state geometry is computed for different amplitudes of the external electric field. The Romberg procedure was also used to remove the higher order hyperpolarizability contaminations. The coupled Hartree-Fock approach provides γ values which account for the self-consistent field-induced modifications of the average electron-electron interactions[36] whereas at the MP2 level, the second-order corrections are included.

The ground state optimized geometrical parameters obtained at both the correlated MP2 and RHF levels of approximation are given in Table I and the normal mode harmonic vibrational frequencies are displayed in Table II.

At the RHF level of approximation when the number of fluorine atoms increases, both the C-H and C-F bond length values decrease whereas experimentally as well as at the MP2 level, only the C-F bond length presents an identical behavior with the hydrogen/fluorine content. The RHF method underestimates the bond lengths by an average amount of 0.014 Å, whereas the MP2-overestimations attain an average of 0.008 Å. Both approaches give bond angle values close to the experimental values.

For the vibrational normal mode frequencies, the MP2 approach substantially reduces the RHF frequency overestimation. In particular, the MP2 frequencies of the modes corresponding to C-F distortions and H-C-H bendings are in perfect agreement with the measured experimental values whereas the C-H stretching frequencies remain overestimated (although to a lesser extent than at the RHF level).

TABLE II. RHF and MP2 harmonic vibrational normal mode frequencies (in cm^{-1} with their irreducible representation) obtained by using the Sadlej basis set in comparison with the measured fundamental frequencies.

	CH_4	CH_3F	CH_2F_2	CHF_3	CF_4
			RHF		
ω_1	1431 (f_2)	1159 (a_1)	581 (a_1)	557 (e)	478 (e)
ω_2	1657 (e)	1286 (e)	1223 (b_2)	768 (a_1)	691 (f_2)
ω_3	3142 (a_1)	1596 (a_1)	1223 (a_1)	1248 (a_1)	1006 (a_1)
ω_4	3272 (f_2)	1600 (e)	1276 (b_1)	1300 (e)	1441 (f_2)
ω_5		3192 (a_1)	1382 (a_2)	1527 (e)	
ω_5		3287 (e)	1577 (b_2)	3333 (a_1)	
ω_7			1648 (a_1)		
ω_8			3246 (a_1)		
ω_9			3320 (b_1)		
			MP2		
ω_1	1315 (f_2)	1055 (a_1)	526 (a_1)	506 (e)	433 (e)
ω_2	1569 (e)	1180 (e)	1094 (b_2)	700 (a_1)	630 (f_2)
ω_3	3035 (a_1)	1470 (a_1)	1113 (a_1)	1141 (a_1)	910 (a_1)
ω_4	3195 (f_2)	1494 (e)	1177 (b_1)	1163 (e)	1283 (f_2)
ω_5		3059 (a_1)	1269 (a_2)	1388 (e)	
ω_5		3178 (e)	1443 (b_2)	3183 (a_1)	
ω_7			1524 (a_1)		
ω_8			3098 (a_1)		
ω_9			3191 (b_1)		
			Experiment[a]		
ω_1	1306 (f_2)	1049 (a_1)	529 (a_1)	507 (e)	435 (e)
ω_2	1535 (e)	1182 (e)	1090 (b_2)	700 (a_1)	631 (f_2)
ω_3	2917 (a_1)	1460 (a_1)	1113 (a_1)	1150 (a_1)	909 (a_1)
ω_4	3019 (f_2)	1468 (e)	1178 (b_1)	1150 (e)	1283 (f_2)
ω_5		2910 (a_1)	1262 (a_2)	1372 (e)	
ω_5		3006 (e)	1435 (b_2)	3036 (a_1)	
ω_7			1508 (a_1)		
ω_8			2948 (a_1)		
ω_9			3014 (b_1)		

[a]The measured vibrational frequencies have been taken from Ref. 1. See references therein for further details.

Inclusion of further electron correlation and of anharmonicity corrections should improve the estimates.

IV. RESULTS AND DISCUSSION

Tables III–VII list the RHF and MP2 mean static second hyperpolarizability terms which contribute in the infinite optical frequency approximation to the vibrational dc-Kerr,

TABLE III. Mean static electronic and vibrational second hyperpolarizability contributions of methane calculated at the RHF and MP2 levels of approximation in comparison with other RHF results. All the values are in atomic units (1.0 a.u. of second hyperpolarizability $=6.235377\times10^{-65}$ C^4 m^4 $J^{-3}=7.0423\times10^{-54}$ m^5 $V^{-2}=5.0367\times10^{-40}$ esu).

CH_4	RHF	MP2	a	b
$\overline{\gamma}^e(0;0,0,0)$	1981.6	2651.1		
$\overline{[\alpha^2]}^{0,0}_{\omega=0}$	760.8	795.0	750.5	679.5
$\overline{[\mu\beta]}^{0,0}_{\omega=0}$	46.0	32.9	37.2	16.4
$\overline{[\mu^2\alpha]}^{1,0}_{\omega=0}$	−6.6	−14.5		−16.2
$\overline{[\mu^2\alpha]}^{0,1}_{\omega=0}$	14.2	−0.2		15.5
$\overline{[\mu^2\alpha]}^{1,0}_{\omega=0}+\overline{[\mu^2\alpha]}^{0,1}_{\omega=0}$	7.6	−14.7	6.62	−0.7

[a]RHF/Sadlej+ results due to Bishop and Dalskov (Ref. 15).
[b]RHF/VTZ2P results due to Luis *et al.* (Ref. 18).

TABLE IV. Mean static electronic and vibrational second hyperpolarizability contributions (in a.u.) of fluoromethane calculated at the RHF and MP2 levels of approximation.

CH_3F	RHF	MP2
$\overline{\gamma^e}(0;0,0,0)$	1341.7	1876.5
$\overline{[\alpha^2]}^{0,0}_{\omega=0}$	622.1	718.9
$\overline{[\mu\beta]}^{0,0}_{\omega=0}$	91.1	174.5
$\overline{[\mu^2\alpha]}^{1,0}_{\omega=0}$	207.1	170.4
$\overline{[\mu^2\alpha]}^{0,1}_{\omega=0}$	211.9	248.0

TABLE V. Mean static electronic and vibrational second hyperpolarizability contributions (in a.u.) of difluoromethane calculated at the RHF and MP2 levels of approximation.

CH_2F_2	RHF	MP2
$\overline{\gamma^e}(0;0,0,0)$	952.3	1461.7
$\overline{[\alpha^2]}^{0,0}_{\omega=0}$	458.6	587.3
$\overline{[\mu\beta]}^{0,0}_{\omega=0}$	53.6	201.1
$\overline{[\mu^2\alpha]}^{1,0}_{\omega=0}$	480.8	589.5
$\overline{[\mu^2\alpha]}^{0,1}_{\omega=0}$	396.4	590.4

TABLE VI. Mean static electronic and vibrational second hyperpolarizability contributions (in a.u.) of fluoroform calculated at the RHF and MP2 levels of approximation.

CHF_3	RHF	MP2
$\overline{\gamma^e}(0;0,0,0)$	734.9	1229.1
$\overline{[\alpha^2]}^{0,0}_{\omega=0}$	323.3	468.0
$\overline{[\mu\beta]}^{0,0}_{\omega=0}$	−31.6	118.2
$\overline{[\mu^2\alpha]}^{1,0}_{\omega=0}$	688.4	962.5
$\overline{[\mu^2\alpha]}^{0,1}_{\omega=0}$	507.3	836.5

TABLE VII. Mean static electronic and vibrational second hyperpolarizability contributions (in a.u.) of tetrafluoromethane calculated at the RHF and MP2 levels of approximation in comparison with other RHF results.

CF_4	RHF	MP2	a
$\overline{\gamma^e}(0;0,0,0)$	502.0	883.5	
$\overline{[\omega^2]}^{0,0}_{\omega=0}$	247.6	407.8	254.7
$\overline{[\mu\beta]}^{0,0}_{\omega=0}$	−67.6	69.2	−66.5
$\overline{[\mu^2\alpha]}^{1,0}_{\omega=0}$	692.2	1028.1	709.9
$\overline{[\mu^2\alpha]}^{0,1}_{\omega=0}$	515.6	905.3	510.5

[a]RHF/VTZ2P results due to Luis *et al.* (Ref. 18).

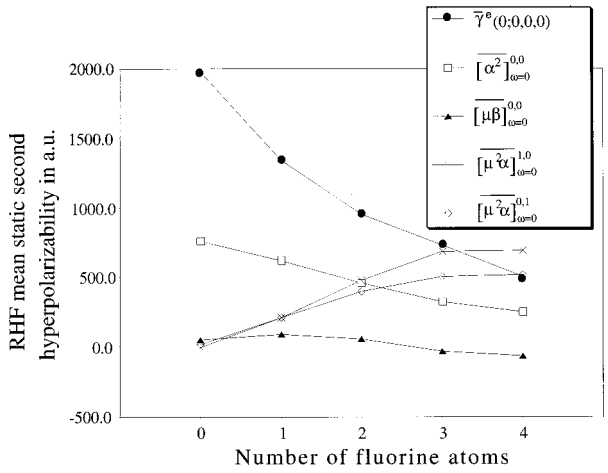

FIG. 1. Evolution with the number of fluorine atoms of the different mean static second hyperpolarizability contributions computed at the RHF level of approximation by using the Sadlej basis set.

ESHG, and DFWM NLO responses. Comparison with the mean static electronic second hyperpolarizability demonstrates that the vibrational contributions become relatively more important as the number of fluorine atoms increases. On the one hand, the RHF values obtained by Luis *et al.*[18] with a smaller basis set are closer to our RHF/Sadlej results for CF_4 than for CH_4. On the other hand for methane, our results are in good agreement with the RHF/Sadlej+ values due to Bishop and co-workers.[14,15]

Systematic trends with the number of fluorine and hydrogen atoms are observed at both levels of approximation (Figs. 1 and 2). With the exception of $\overline{[\mu\beta]}^{0,0}_{\omega=0}$, good linear regressions characterize the evolution of the different second hyperpolarizability terms as a function of the number of fluorine atoms; the correlation coefficients of the least-squares fitting are larger than 0.95. This fact extends the validity of the bond-additivity scheme to the vibrational second hyperpolarizability. Ward and Bigio[3] were the first to demonstrate

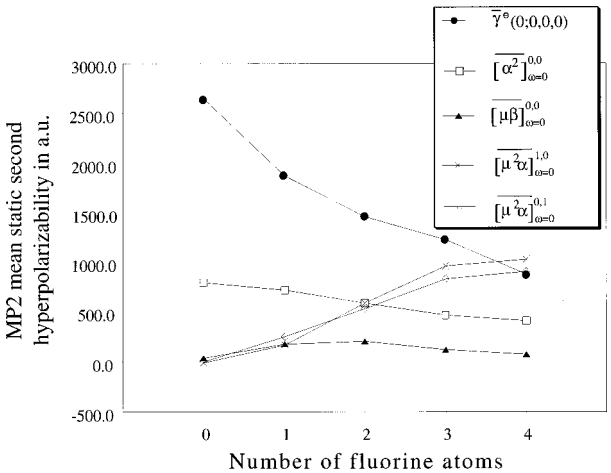

FIG. 2. Evolution with the number of fluorine atoms of the different mean static second hyperpolarizability contributions computed at the MP2 level of approximation by using the Sadlej basis set.

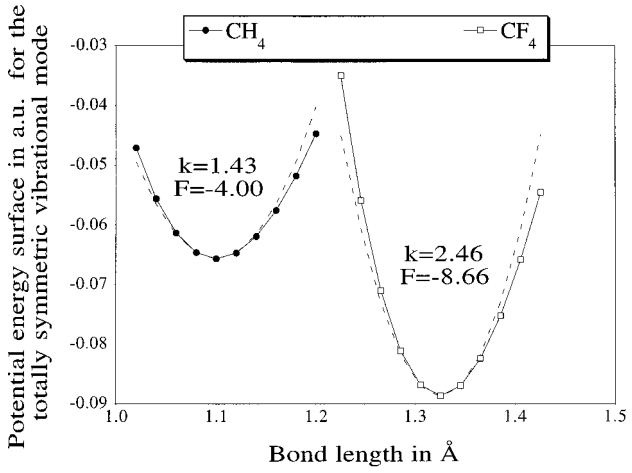

FIG. 3. MP2/Sadlej nuclear potential for the totally symmetric stretching mode of CH_4 and CF_4. Dashed lines represent the harmonic potential. The harmonic force constants, $k=\partial^2 E/\partial R^2$, and the anharmonicity cubic force constants, $F=\partial^3 E/\partial R^3$, which have been obtained by fitting the data points to a polynomial of third order in the bond displacements, are in very close agreement with the computed quantities. All values except the distances (in Å) are given in a.u. The energy values have been shifted by 40.3 a.u. and 436.6 a.u. for CH_4 and CF_4, respectively.

the usefulness of bond additivity for the electronic second hyperpolarizability of fluorinated methanes whereas bond additivity does not work for β^e (Refs. 3 and 4) just as it does not for $\overline{[\mu\beta]}^{0,0}_{\omega=0}$. The larger the number of hydrogen atoms, the larger the $\overline{\gamma^e}(0;0,0,0)$ and $\overline{[\alpha^2]}^{0,0}_{\omega=0}$ values but the smaller the $\overline{[\mu^2\alpha]}^{1,0}_{\omega=0}$ and $\overline{[\mu^2\alpha]}^{0,1}_{\omega=0}$ contributions. $\overline{[\mu\beta]}^{0,0}_{\omega=0}$ is much smaller than $\overline{[\alpha^2]}^{0,0}_{\omega=0}$, $\overline{[\mu^2\alpha]}^{1,0}_{\omega=0}$ and $\overline{[\mu^2\alpha]}^{0,1}_{\omega=0}$ and is maximum either for CH_3F (RHF) or for CH_2F_2 (MP2).

In comparison, the CHF static electronic average polarizability, $\overline{\alpha^e}(0;0)$, is equal to 16.0, 15.6, 15.7, 16.1, and 16.5 a.u. for CH_4, CH_3F, CH_2F_2, CH_3F, and CF_4, respectively, whereas at the FF/MP2 level it increases slightly and attains 16.9, 17.1, 17.8, 18.7, and 19.4 a.u. With the exception of the CHF result for methane, the linear electronic polarizability increases with the number of fluorine atoms (the opposite trend to the electronic second hyperpolarizability). Obviously, the variation of polarizability follows the number of electrons or the van der Waals volume of the molecule whereas the second hyperpolarizability substantially decreases with the ionic character of the bonds.

The variations in $\overline{[\alpha^2]}^{0,0}_{\omega=0}$—as well as in the other vibrational terms—are related to the changes of vibrational frequencies and polarizability derivatives with respect to the normal coordinates [Eq. (4)]. The alternative representation of $\overline{[\alpha^2]}^{0,0}_{\omega=0}$ using internal vibrational coordinates,

$$[\alpha^2]^{0,0}_{\omega=0}=3\sum_{i,j}\left(\frac{\partial\alpha^e_{\zeta\eta}}{\partial R_i}\right)_0(\mathbf{F}^{-1})_{ij}\left(\frac{\partial\alpha^e_{\xi\chi}}{\partial R_j}\right)_0 \tag{12}$$

enables an easier interpretation. $\mathbf{F}^{-1}$ is the inverse of the vibrational force constant matrix. The decrease of $\overline{[\alpha^2]}^{0,0}_{\omega=0}$ with the content in fluorine atoms is explained by the much steeper potential energy surface associated with the C-F bonds and therefore to a larger force constant. This is represented in Fig. 3 for the totally-symmetric (a_1) stretching mode of CH_4 and CF_4 at the MP2 level of approximation. To be rigorously correct, one should also consider the $(\partial\alpha^e_{\zeta\eta}/\partial R_i)_0$ terms associated with the other stretching and bending modes. However, in a first approximation it is sufficient to consider only the a_1 mode since it presents the largest contribution to $\overline{[\alpha^2]}^{0,0}_{\omega=0}$. These curves show also that the C-F bonds have larger anharmonic force constants than their hydrogenated analogs and this is consistent with their larger $\overline{[\mu^2\alpha]}^{0,1}_{\omega=0}$ terms.

The sum of these first-order mechanical and electrical anharmonicity terms, $\overline{[\mu^2\alpha]}^{I}_{\omega=0}=\overline{[\mu^2\alpha]}^{1,0}_{\omega=0}+\overline{[\mu^2\alpha]}^{0,1}_{\omega=0}$, is quantitatively important with respect to both γ^e and the other vibrational terms. Nevertheless, in the infinite frequency approximation it only contributes to the dc-Kerr response. At the RHF level, $\overline{[\mu^2\alpha]}^{I}$ contributes 0.5%, 21.6%, 44.9%, 68.4%, and 80.5% to the total $\overline{\gamma^v}(-\omega;\omega,0,0)$ value for CH_4, CH_3F, CH_2F_2, CHF_3, and CF_4, respectively whereas at the MP2 level, the contribution percentages are slightly smaller; −0.9%, 17.6%, 39.9%, 58.2%, and 65.4%. Similar values are obtained when considering the anisotropic Kerr constant.

The behavior of the $\overline{[\mu\beta]}^{0,0}_{\omega=0}$ term with the nature of the system is more difficult. The MP2 results suggest that it increases with the molecular asymmetry; CH_4 and CF_4 belong to T_d, CH_3F and CHF_3 to C_{3v} while CH_2F_2 belongs to C_{2v} point groups. An explanation of this behavior probably requires going beyond the bond-additivity scheme and considering the bond-bond interactions as proposed by Miller and Ward for explaining the variation in β^e.[4]

The effect of including electron correlation leads to systematic augmentation of $\overline{\gamma^e}(0;0,0,0)$, $\overline{[\alpha^2]}^{0,0}_{\omega=0}$, $\overline{[\mu^2\alpha]}^{1,0}_{\omega=0}$ (except CH_3F) and $\overline{[\mu^2\alpha]}^{0,1}_{\omega=0}$. These correlation-induced augmentations increase with the number of fluorine atoms. Although it is not the purpose of this study, it is comforting to see that the MP2 corrections to $\overline{\gamma^e}(0;0,0,0)$ for CH_4 and CF_4 go in the same direction as in other studies including those which include more electron correlation.[17,37,38] A comparison with experiment of the total γ values requires taking into account the frequency dependence of γ^e for the different NLO processes and this is beyond the scope of this study since no frequency-dependent calculations were made for γ^e.

Tables VIII– XII list the vibrational mean second hyperpolarizability contribution for the dc-Kerr, ESHG, and DFWM phenomena and the anisotropic Kerr constant in the infinite optical frequency approximation in comparison with the values obtained by considering the frequency-dependence according to Eqs. (3)–(7) with $\hbar\omega=0.072E_h=1.96$ eV (which corresponds to $\lambda=6328$ Å). When γ^v is non-negligible with respect to γ^e, i.e., for dc-Kerr and DFWM processes, the replacement of $\hbar\omega=0.072\,E_h$ by $\omega\rightarrow\infty$ leads to a small increase of γ^v. The maximum increase (16.6%) occurs for the MP2 $\gamma^{v,K}(-\omega;\omega,0,0)$ of CH_4, whereas in most cases the overestimation is less than 5%. For ESHG, the small γ^v values vary substantially be-

TABLE VIII. Vibrational contributions to the mean (dc-Kerr, ESHG, DFWM) and anisotropic (dc-Kerr) dynamic second hyperpolarizability of methane (in a.u.). The infinite optical frequency vibrational second hyperpolarizability values ($\omega\rightarrow\infty$) are compared to the corresponding dynamic values obtained from Eqs. (3)–(7) with $\lambda=6328$ Å.

	RHF		MP2					
CH_4	$\omega\rightarrow\infty$	$\lambda=6328$ Å	$\omega\rightarrow\infty$	$\lambda=6328$ Å	a $\omega\rightarrow\infty$	b $\omega\rightarrow\infty$	b $\lambda=6328$ Å	c $\omega\rightarrow\infty$
$\overline{\gamma}^{v}(-\omega;\omega,0,0)$	277.8	256.3	279.0	258.7	269.9	300.1	276.4	234.6
$\overline{\gamma}^{v}(-2\omega;\omega,\omega,0)$	11.5	−12.6	8.2	−14.5	9.3	11.6	−15.0	4.1
$\overline{\gamma}^{v}(-\omega;\omega,-\omega,\omega)$	507.2	501.7	530.0	525.5	500.3	551.5	545.6	453.0
$\gamma^{v,K}(-\omega;\omega,0,0)$	168.8	163.3	170.3	146.1	178.6	202.2	174.2	160.7

[a](B)-RHF/Sadlej+ results due to Bishop and Dalskov (Ref. 15). (B) corresponds to the nuclear relaxation approximation where only the lowest-order terms of each type are taken into account.
[b](C)-RHF/Sadlej+ results due to Bishop and Dalskov (Ref. 15). Method (C) includes contributions through second-order in electrical, and first-order in mechanical, anharmonicity (except second-order terms involving the third derivatives of the electronic properties).
[c]RHF/VTZ2P results due to Luis *et al.* (Ref. 18) obtained with the nuclear relaxation/infinite frequency method.

tween the two methods. Similarly to Bishop and Dalskov[15] we find a change of sign for $\overline{\gamma}^{v}(-2\omega;\omega,\omega,0)$ of CH_4. The variations are also substantial for CH_3F and CH_2F_2 particularly at the RHF level. In the infinite optical frequency approximation, the variations in $\overline{\gamma}^{v}(-\omega_\sigma;\omega_1,\omega_2,\omega_3)$ as a function of the number of fluorine atoms and as a function of the method are explained by weighing the variations of their contributing terms according to Eqs. (8)–(11). Since the $\omega\rightarrow\infty$ approximation is valid when γ^{v} is of importance, such a weighing procedure also explains the variations when considering $\lambda=6328$ Å. As a consequence, CH_4 presents the largest DFWM γ^{v} response which at the MP2 level reaches 19.8% of $\overline{\gamma}^{e}(0;0,0,0)$ ($\lambda=6328$ Å). The $\overline{\gamma}^{v}(-\omega;\omega,-\omega,\omega)$ of CH_3F is also important and is 25.2% of $\overline{\gamma}^{e}(0;0,0,0)$ within the same approach. For CH_2F_2, CHF_3, and CF_4 the increasing contribution, with respect to the fluorine content, of the anharmonic $[\mu^2\alpha]^{I}_{\omega=0}$ term accounts for the fact that the dc-Kerr responses exhibit the largest γ^{v} component. For these three molecules given in the same order, the $\overline{\gamma}^{v}(-\omega;\omega,0,0)/\overline{\gamma}^{e}(0;0,0,0)$ ratio amounts to 0.327, 0.411, and 0.526 at the MP2 level with $\lambda=6328$ Å. In all cases, the ESHG vibrational contribution is small as a result of the small $\overline{[\mu\beta]}^{0,0}_{\omega=0}$ terms.

Both $\gamma^{v,K}(-\omega;\omega,0,0)$ and $\overline{\gamma}^{v}(-2\omega;\omega,\omega,0)$ are necessary in order to deduce either the ESHG or dc-Kerr total second hyperpolarizability values from the dispersion curve of the other one—if one can assume negligible dispersions for $\gamma^{v,K}(-\omega;\omega,0,0)$ and $\overline{\gamma}^{v}(-2\omega;\omega,\omega,0)$ only their difference is required.[12] In fact, at high optical frequency, the difference between the anisotropic dc-Kerr and mean ESHG vibrational second hyperpolarizabilities, $\Delta=\gamma^{v,K}(-\omega;\omega,0,0)-\overline{\gamma}^{v}(-2\omega;\omega,\omega,0)$, is approximately frequency-independent and tends towards a constant value. Δ can therefore be obtained from the knowledge of both the ESHG and dc-Kerr dispersion curves while taking care, if necessary, of its dispersion. The Δ value of CH_4 determined by Shelton and Palubinskas[12] is obtained from their dc-Kerr data points and the fit to their ESHG data points whereas their value of Δ (CF_4) corresponds to $\lambda=6328$ Å. For $\omega\rightarrow\infty$ and $\hbar\omega=0.072\ E_h$ ($\lambda=6328$ Å), we have then calculated the Δ values at both the RHF and MP2 levels of approximation (Table XIII). The RHF and MP2 Δ values are similar and are in close agreement with the other theoretical values calculated at the same level of approximation. The Δ values calculated by Bishop and co-workers[14,15] which include higher-order anharmonicity corrections (denoted C in Ref. 15) show however a slight improvement. For CF_4, the MP2 Δ value is in good agreement with the experimentally-derived data. In fact, with the exception of methane, both electron correlation and anharmonicity contribute signifi-

TABLE IX. Vibrational contributions to the mean (dc-Kerr, ESHG, DFWM) and anisotropic (dc-Kerr) dynamic second hyperpolarizability of fluoromethane (in a.u.). The infinite optical frequency vibrational second hyperpolarizability values ($\omega\rightarrow\infty$) are compared to the corresponding dynamic values obtained from Eqs. (3)–(7) with $\lambda=6328$ Å.

	RHF		MP2	
CH_3F	$\omega\rightarrow\infty$	$\lambda=6328$ Å	$\omega\rightarrow\infty$	$\lambda=6328$ Å
$\overline{\gamma}^{v}(-\omega;\omega,0,0)$	322.8	304.5	396.6	378.6
$\overline{\gamma}^{v}(-2\omega;\omega,\omega,0)$	22.8	3.5	43.6	24.3
$\overline{\gamma}^{v}(-\omega;\omega,-\omega,\omega)$	414.7	408.9	479.3	473.8
$\gamma^{v,K}(-\omega;\omega,0,0)$	276.5	255.2	329.9	308.7

TABLE X. Vibrational contributions to the mean (dc-Kerr, ESHG, DFWM) and anisotropic (dc-Kerr) dynamic second hyperpolarizability of difluoromethane (in a.u.). The infinite optical frequency vibrational second hyperpolarizability values ($\omega\rightarrow\infty$) are compared to the corresponding dynamic values obtained from Eqs. (3)–(7) with $\lambda=6328$ Å.

	RHF		MP2	
CH_2F_2	$\omega\rightarrow\infty$	$\lambda=6328$ Å	$\omega\rightarrow\infty$	$\lambda=6328$ Å
$\overline{\gamma}^{v}(-\omega;\omega,0,0)$	325.8	312.3	493.0	478.7
$\overline{\gamma}^{v}(-2\omega;\omega,\omega,0)$	13.4	0.2	50.3	36.1
$\overline{\gamma}^{v}(-\omega;\omega,-\omega,\omega)$	305.7	301.2	391.5	386.7
$\gamma^{v,K}(-\omega;\omega,0,0)$	312.4	296.8	455.7	439.2

TABLE XI. Vibrational contributions to the mean (dc-Kerr, ESHG, DFWM) and anisotropic (dc-Kerr) dynamic second hyperpolarizability of fluoroform (in a.u.). The infinite optical frequency vibrational second hyperpolarizability values ($\omega\rightarrow\infty$) are compared to the corresponding dynamic values obtained from Eqs. (3)–(7) with $\lambda = 6328$ Å.

	RHF		MP2	
CHF_3	$\omega\rightarrow\infty$	$\lambda = 6328$ Å	$\omega\rightarrow\infty$	$\lambda = 6328$ Å
$\overline{\gamma}^{\nu}(-\omega;\omega,0,0)$	291.3	283.0	514.9	505.3
$\overline{\gamma}^{\nu}(-2\omega;\omega,\omega,0)$	−7.9	−15.0	29.5	21.1
$\overline{\gamma}^{\nu}(-\omega;\omega,-\omega,\omega)$	215.5	213.7	312.0	309.3
$\gamma^{\nu,K}(-\omega;\omega,0,0)$	293.0	283.6	491.6	480.6

TABLE XII. Vibrational contributions to the mean (dc-Kerr, ESHG, DFWM) and anisotropic (dc-Kerr) dynamic second hyperpolarizability of tetrafluoromethane (in a.u.). The infinite optical frequency vibrational second hyperpolarizability values ($\omega\rightarrow\infty$) are compared to the corresponding dynamic values obtained from Eqs. (3)–(7) with $\lambda = 6328$ Å.

	RHF		MP2		a
CF_4	$\omega\rightarrow\infty$	$\lambda = 6328$ Å	$\omega\rightarrow\infty$	$\lambda = 6328$ Å	$\omega\rightarrow\infty$
$\overline{\gamma}^{\nu}(-\omega;\omega,0,0)$	250.0	246.3	492.7	464.8	255.1
$\overline{\gamma}^{\nu}(-2\omega;\omega,\omega,0)$	−16.9	−19.1	17.3	13.8	−16.6
$\overline{\gamma}^{\nu}(-\omega;\omega,-\omega,\omega)$	165.1	165.0	271.8	271.4	169.8
$\gamma^{\nu,K}(-\omega;\omega,0,0)$	252.6	248.3	463.6	457.6	265.8

[a]RHF/VTZ2P results due to Luis *et al.* (Ref. 18) obtained with the nuclear relaxation/infinite frequency method.

cantly to Δ as well as to the various vibrational second hyperpolarizabilities. Moreover, as could have been expected from the previous paragraph, the $\omega\rightarrow\infty$ approximation works also nicely for estimating Δ. Since for CH_4 the MP2/infinite frequency quantity remains far from the experimental value whereas for CF_4 it is in rather good agreement, it would be interesting to know how the theoretical values for CH_3F, CH_2F_2, and CHF_3 match the experiment.

V. CONCLUSIONS

The frequency-dependent vibrational second hyperpolarizability of the $CH_{4-n}F_n$ molecules with $n = 0-4$ has been computed for the most common NLO processes by adopting the perturbation approach due to Bishop and Kirtman.[7,22] Systematic variations of the different γ contributions have been obtained with respect to the number of hydrogen (fluorine) atoms. Analysis of the potential energy surface of the C-H and C-F bonds has enabled us to understand some of these γ variations. To our knowledge this is one of the few times (other correlated investigations are given in Refs. 17, 39 and 40) that calculations of the mean vibrational second hyperpolarizability including anharmonicity corrections have been carried out consistently at a correlated level (MP2) for polyatomic molecules. It turns out that electron correlation effects on the various γ contributions are important in many instances and increase with the number of fluorine atoms. The anharmonic contribution to the dc-Kerr responses is large and, in addition, it dominates the vibrational response of CHF_3 and CF_4. With the evidence at hand, we conclude also that the infinite optical frequency method is a satisfactory approximation for evaluating the vibrational NLO responses. The striking result of this study is the good agreement between the MP2 and the experimental value for the difference between the vibrational dc-Kerr and ESHG hyperpolarizability of CF_4. Nevertheless, even if electron correlation effects and anharmonicity corrections are considered simultaneously, our approach remains insufficient in the case of CH_4. In order to close the gap between the experimental and theoretical results we are currently extending our approach by including explicitly dispersion effects in the perturbation approach due to Bishop and Kirtman.[7,22] Indeed, in this method, one ignores the dispersion of the $(\partial P^e/\partial Q_a)_0$ and $(\partial^2 P^e/\partial Q_a \partial Q_b)_0$ quantities.

ACKNOWLEDGMENTS

The authors are pleased to acknowledge Professor D. M. Bishop for a careful reading of the manuscript, as well as Professor J. M. André, Professor B. Kirtman, Professor D. M. Bishop, Dr. E. A. Perpète, and J. Luis for stimulating discussions. B.C. thanks the Belgian National Fund for Scientific Research for his Research Associate position. The cal-

TABLE XIII. Comparison of the experimentally derived differences between the anisotropic dc-Kerr and ESHG values, $\Delta = \gamma^{\nu,K}(-\omega;\omega,0,0) - \overline{\gamma}^{\nu}(-2\omega;\omega,\omega,0)$, determined by Shelton and Palubinskas (Ref. 12) to the calculated values obtained at both the RHF and MP2 levels of approximation. All the values are given in a.u.

	RHF		MP2		Other theoretical work		
	$\omega\rightarrow\infty$	$\lambda = 6328$ Å	$\omega\rightarrow\infty$	$\lambda = 6328$ Å	$\omega\rightarrow\infty$	$\lambda = 6328$ Å	Expt.[d]
CH_4	157.3	175.9	162.1	160.6	169.3[a]		289
					190.6[b]	189.2[b]	
					156.6[c]		
CH_3F	254.2	251.7	286.4	284.4			
CH_2F_2	299.0	296.6	405.4	403.1			
CHF_3	300.9	298.6	462.1	459.5			
CF_4	269.0	267.4	446.3	443.8	282.4[c]		497

[a](B)-RHF/Sadlej+ results due to Bishop and Dalskov (Ref. 15).
[b](C)-RHF/Sadlej+ results due to Bishop and Dalskov (Ref. 15).
[c]RHF/VTZ2P results due to Luis *et al.* (Ref. 18).
[d]Reference 12.

culations have been performed on the IBM SP2 of the Namur Scientific Computing Facility (Namur-SCF). The authors gratefully acknowledge the financial support of the FNRS-FRFC, the ''Loterie Nationale'' for the convention No. 2.4519.97 and the Belgian National Interuniversity Research Program on ''Sciences of Interfacial and Mesoscopic Structures'' (PAI/IUAP No. P4/10).

[1] D. S. Elliott and J. F. Ward, Mol. Phys. **51**, 45 (1984).
[2] J. F. Ward and D. S. Elliott, J. Chem. Phys. **80**, 1003 (1984).
[3] J. F. Ward and I. J. Bigio, Phys. Rev. A **11**, 60 (1975).
[4] C. K. Miller and J. F. Ward, Phys. Rev. A **16**, 1179 (1977).
[5] A. D. Buckingham and B. J. Orr, Trans. Faraday Soc. **65**, 673 (1969).
[6] D. P. Shelton and A. D. Buckingham, Phys. Rev. A **26**, 2787 (1982).
[7] D. M. Bishop and B. Kirtman, J. Chem. Phys. **95**, 2646 (1991).
[8] D. M. Bishop, M. Hasan, and B. Kirtman, J. Chem. Phys. **103**, 4157 (1995).
[9] D. P. Shelton, Phys. Rev. A **34**, 304 (1986).
[10] Z. Lu and D. P. Shelton, J. Chem. Phys. **87**, 1967 (1987).
[11] D. P. Shelton, Phys. Rev. A **42**, 2578 (1990).
[12] D. P. Shelton and J. J. Palubinskas, J. Chem. Phys. **104**, 2482 (1996).
[13] J. Martí, J. L. Andrés, J. Bertrán, and M. Duran, Mol. Phys. **80**, 625 (1993).
[14] D. M. Bishop and J. Pipin, J. Chem. Phys. **103**, 4980 (1995).
[15] D. M. Bishop and E. K. Dalskov, J. Chem. Phys. **104**, 1004 (1996).
[16] D. M. Bishop and S. P. A. Sauer, J. Chem. Phys. **107**, 8502 (1997).
[17] J. M. Luis, J. Martí, M. Duran, and J. L. Andrés, Chem. Phys. **217**, 29 (1997).
[18] J. M. Luis, J. Martí, M. Duran, J. L. Andrés, and B. Kirtman, J. Chem. Phys. **108**, 4123 (1998).
[19] P. Norman, Ph.D. thesis, Nonlinear Optical Properties of Fullerenes, Oligomers, and Solutions, Linköping, 1998, Chap. 19.
[20] D. M. Bishop, B. Kirtman, and B. Champagne, J. Chem. Phys. **107**, 5780 (1997).
[21] J. Martí and D. M. Bishop, J. Chem. Phys. **99**, 3860 (1993).
[22] D. M. Bishop, J. M. Luis, and B. Kirtman, J. Chem. Phys. **108**, 10013 (1998).
[23] D. M. Bishop and D. W. De Kee, J. Chem. Phys. **104**, 9876 (1996).
[24] D. M. Bishop and D. W. De Kee, J. Chem. Phys. **105**, 8247 (1996).
[25] C. Hättig, Mol. Phys. **94**, 455 (1998).
[26] D. M. Bishop, Adv. Chem. Phys. **104**, 1 (1998).
[27] B. Kirtman and B. Champagne, Int. Rev. Phys. Chem. **16**, 389 (1997).
[28] GAUSSIAN 94, Revision B.1, M. J. Frisch, G. W. Trucks, H. B. Schlegel, P. M. W. Gill, B. G. Johnson, M. A. Robb, J. R. Cheeseman, T. Keith, G. A. Petersson, J. A. Montgomery, K. Raghavachari, M. A. Al-Laham, V. G. Zakrzewski, J. V. Ortiz, J. B. Foresman, J. Cioslowski, B. B. Stefanov, A. Nanayakkara, M. Challacombe, C. Y. Peng, P. Y. Ayala, W. Chen, M. W. Wong, J. L. Andres, E. S. Replogle, R. Gomperts, R. L. Martin, D. J. Fox, J. S. Binkley, D. J. Defrees, J. Baker, J. P. Stewart, M. Head-Gordon, C. Gonzalez, and J. A. Pople, Gaussian, Inc., Pittsburgh, Pennsylvania, 1995.
[29] A. J. Sadlej, Collect. Czech. Chem. Commun. **53**, 1995 (1988); Theor. Chim. Acta **79**, 123 (1992); K. Andersson and A. J. Sadlej, Phys. Rev. A **46**, 2356 (1992).
[30] O. Quinet and B. Champagne (unpublished results).
[31] See, for example, Y. Yamaguchi, Y. Osamura, J. D. Goddard, and H. F. Schaefer III, *A New Dimension to Quantum Chemistry: Analytic Derivative Methods in Ab Initio Molecular Electronic Structure Theory* (Oxford University Press, Oxford, 1994).
[32] P. J. Davis and P. Rabinowitz, *Numerical Integration* (Blaisdell, London, 1967), p. 166.
[33] B. Champagne, Chem. Phys. Lett. **261**, 57 (1996).
[34] H. D. Cohen and C. C. J. Roothaan, J. Chem. Phys. **43**, S34 (1965).
[35] O. Quinet (unpublished results).
[36] P. W. Langhoff, M. Karplus, and R. P. Hurst, J. Chem. Phys. **44**, 505 (1966); T. C. Caves and M. Karplus, *ibid.* **50**, 3649 (1969).
[37] G. Maroulis, Chem. Phys. Lett. **226**, 420 (1994).
[38] G. Maroulis, Chem. Phys. Lett. **259**, 654 (1996).
[39] D. M. Bishop, B. Kirtman, H. A. Kurtz, and J. E. Rice, J. Chem. Phys. **98**, 8024 (1993).
[40] D. M. Bishop, J. Pipin, and B. Kirtman, J. Chem. Phys. **102**, 6778 (1995).